

Finite Element Analysis of Steel Deep Beam-to-Column Connections with Web Opening

*Sun-hoon Kim¹⁾ Keunyeong Oh²⁾ Chang-hoon Kang³⁾ and Kangmin Lee⁴⁾

^{1,4)} Department of Architectural Engineering, Chungnam National University, Daejeon 305-764, Korea

²⁾ Korea Institute of Civil Engineering and Building Technology, Goyang 102-223, Korea

³⁾ Hyundai Engineering, Seoul 03134, Korea

¹⁾ gns0712@naver.com

²⁾ oky88@kict.re.kr

³⁾ judeman@hec.co.kr

⁴⁾ leekm@cnu.ac.kr

ABSTRACT

Recently, the demand for deep steel beams has been increasing in the construction industry due to buildings becoming bigger and taller. This study aims to evaluate the structural performance of a beam-to-column steel connection in deep beams with different beam depths and web opening shapes, via modeling with finite element analysis (FEA). The load and accumulated energy dissipation rate from the experimental and the FEA results were found comparable, validating the developed model. The beam model with a rectangular web opening showed the highest equivalent plastic strain (PEEQ) values at the end of the beam, whereas the one with a circular opening showed the highest PEEQ values around the web opening. All samples satisfied the performance requirements outlined by Korea Design Standard (KDS) and Special Moment Frame (SMF). In addition, creating plastic hinges through web openings was deemed suitable.

1. INTRODUCTION

Recently, the demand for steel and composite beams has been increasing in the Korean construction market due to buildings becoming bigger and taller. As a result, demand for the beams with larger beam depth has also risen. Therefore, in this study, based on the results from the hysteretic behavior experiments on full-size beam to column connections, the structural characteristics of samples were analyzed through modeling with a

¹⁾ Graduate Student

²⁾ Ph.D

³⁾ Ph.D

⁴⁾ Professor

nonlinear FEA program called ABAQUS.

1. EXPERIMENTAL PROCEDURE AND SUMMARY OF RESULTS

As shown in Figure 1, the samples were designed to have a beam-to-column connection in a 'T' shape, with both ends of the columns set as hinges and the load applied at the end of the beam via a displacement-controlled loading method. The RO (Rectangular Opening) sample was designed with a rectangular opening for duct use, whereas the CRO (Circular + Rectangular Opening) samples were designed with both circular and rectangular openings, with the circular opening for inducing plastic hinge and rectangular opening for duct use. The samples yielded at both top and bottom flanges of the beam at 1.5% lateral drift, and at the beam web at 3%. Subsequently, local buckling occurred at the flange and web of the beam at a lateral drift of 4%. In addition, a lateral torsion was caused due to buckling at 5%. For rectangular web openings in pipes, buckling or torsion was not observed. The initial stiffness for CRO and RO was 9.54 kN/mm and 9.80 kN/mm, respectively. The maximum load was measured at 4% lateral drift before local buckling occurred

Table 1. Dimensionless moment – Story drift ratio

Names	Positive (+)		Negative (-)	
	M/M _p	Story drift ratio(θ)	M/M _p	Story drift ratio(θ)
CRO	1.43	0.0362	1.48	0.0370
RO	1.37	0.0401	1.40	0.0381

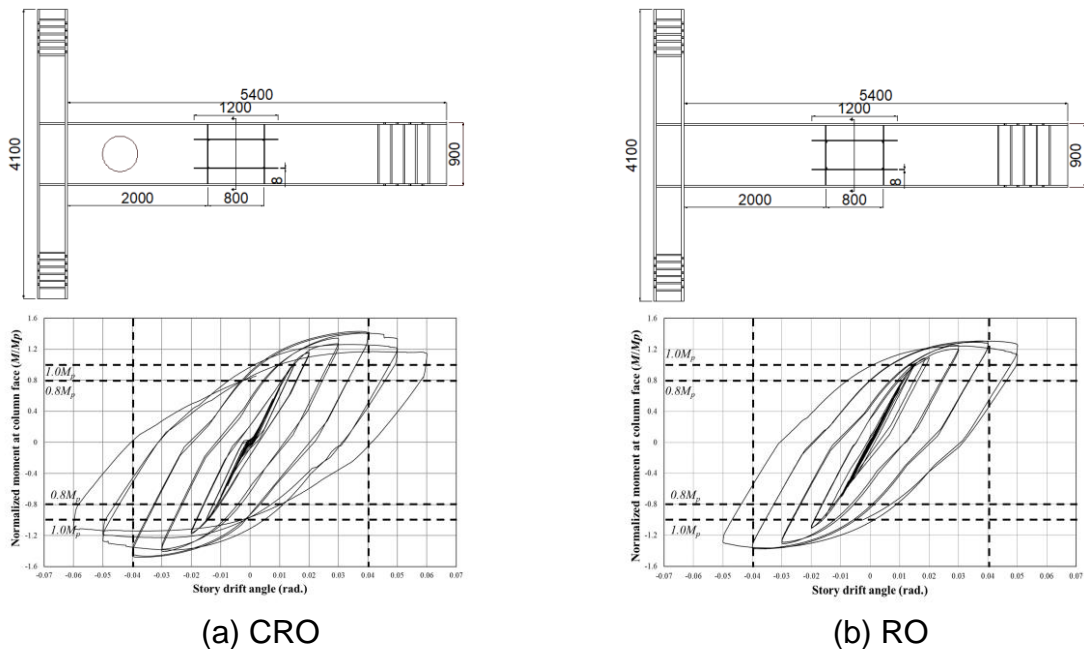


Figure 1. Schematic of test

3. FINITE ELEMENT MODELING

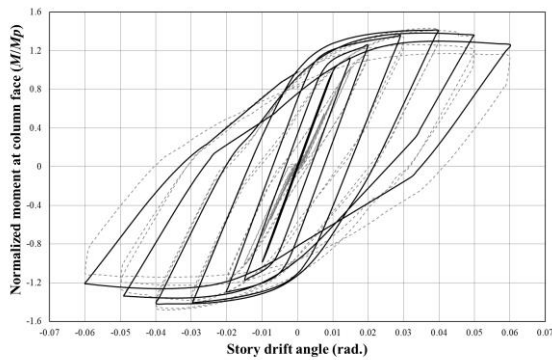
ABAQUS / CAE 6.13 was used for the FEA. Material property values were obtained experimentally. For analysis with ABAQUS, the engineering stress and strain values had to be converted to true stress and strain values. This was completed using the following two equations.

$$\sigma_{true} = \sigma_{eng} (1 + \varepsilon_{eng}) \quad (1)$$

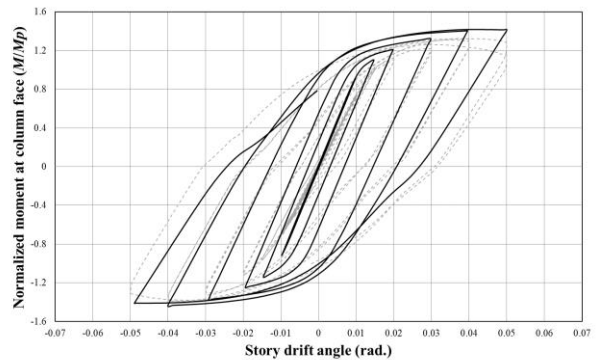
$$\varepsilon_{ln}^{p l} = \ln(1 + \varepsilon_{eng}) - \frac{\sigma_{true}}{E} \quad (2)$$

where σ_{true} , σ_{eng} , $\varepsilon_{ln}^{p l}$, and ε_{eng} denote true stress, engineering stress, true strain, and engineering strain, respectively.

The modeling of beam-to-column connections was accomplished using ABAQUS three-dimensional solid element with eight nodes (C3D8R) to consider large deformations. The analysis was conducted under the same support conditions as the experiment, with the load applied to the samples according to the experimental cyclic loading procedures. However, due to the limited analysis time, the load was applied for one cycle per lateral drift using the displacement-controlled loading method.



(a) CRO



(b) RO

Figure 2 shows a comparison of experimental and FEA results. The initial stiffness was quite high, but it is believed to be an error due to experimental setup and slip. However, similarities between buckling, point of maximum load, and point of load reduction from experimental and analysis results were noted, which suggested that the developed finite element models are reliable

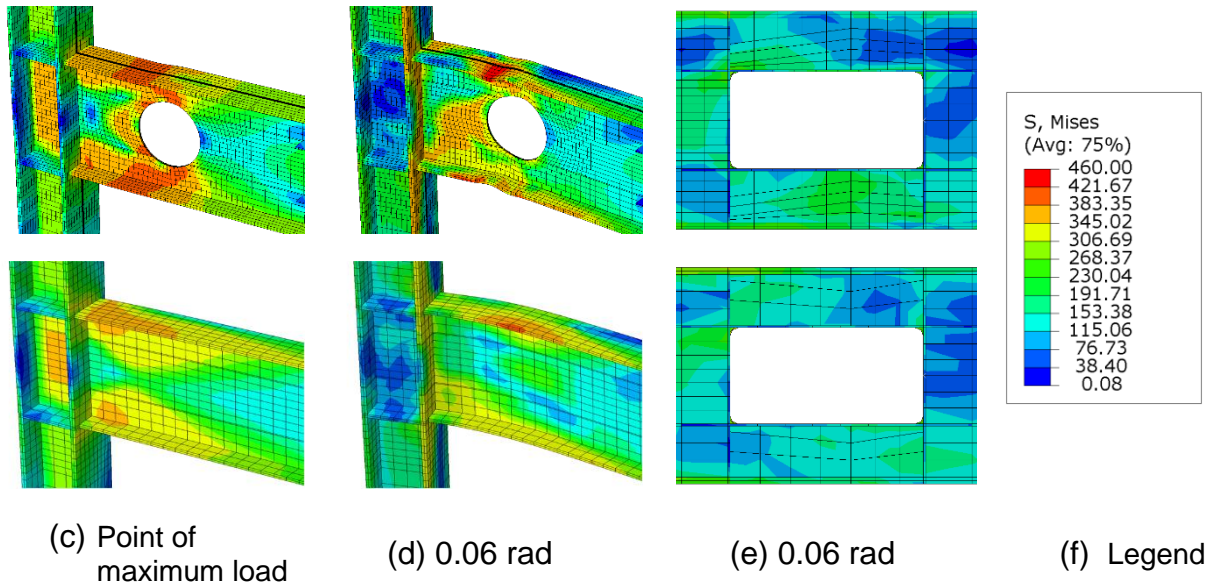


Figure 3. von Mises stress distributions

Figure 3 shows the von Mises stress distributions for FEA models. Hysteretic behavior of the models appeared to be similar during the experiments. As shown in Figure 2, a stress concentration around the web opening was observed in the model with circular web opening and a flange deformation was observed at the concentrated stress location. For the model with rectangular web opening, no concentration of stress was observed around the web opening, but a stress concentration on the flange at the end of the beam was observed.

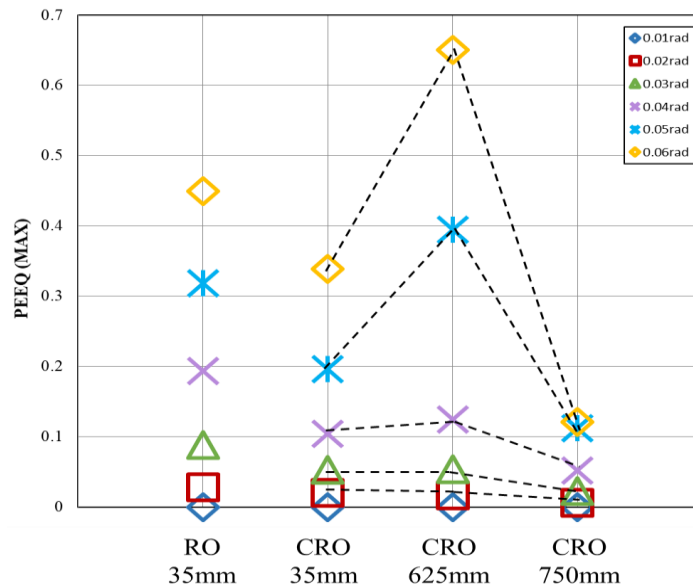


Figure 4. PEEQ distribution at ends of the beams in each finite element model

To verify the occurrence of brittle fractures, PEEQ distribution was examined. If a welded connection exists at a point with concentrated stress, possibility of fracture increases. Therefore, PEEQ values at 35 mm from the end of the beam and at locations estimated to have maximum PEEQ at the circular web openings were obtained, as shown in Figure 3. For both finite element models, PEEQ values were shown to increase starting from 0.04 rad., which is the point of maximum load. From the two samples, CRO showed a larger increase in PEEQ than RO. This may be due to the flange deformation at the circular web opening during peak loading conditions. In contrast, PEEQ value at the end of the beam was less than that of RO model, suggesting that plastic hinge was induced through the circular web opening.

4. CONCLUSIONS

In this study, the reliability of finite element models of beams was verified using experimental results for deep beams with web openings. The structural characteristics of the hysteretic behavior were analyzed, and the suitability of beam design was examined. Based on this, the following conclusions were drawn

- (1) Given the stress distributions and PEEQ values, there was no concentration of stress or deformation for beams with rectangular web opening. Therefore, using rectangular web openings for facilities and ducting purposes is deemed safe.
- (2) Circular web openings are designed to induce a plastic hinge at the estimated plastic hinge location. For the CRO model, stress concentration was observed mostly at the web opening but not as much at the end of the beam. Hence, circular web openings can prevent brittle fractures. Hence, they can be used to induce plastic hinges.

REFERENCES

- Park, J.W., Kang, S.M., Hwang, I.K., Kang, T.K., Kwon, K.J. (2001), "Behavior of Reduced Beam Section Connections with Web Openings", *KSSC.*, **13**(2). 395-405
- Kim, J.H., Kim, H.C., Jeong, J.H., Kim, J.M., Joo, K.J. (2000), "A Study on the Reinforcing Efficiency of H-shaped Steel Beams with a rectangular Web opening by F.E.M analysis", *AIOK.*, **20**(2) 11-14
- Heo, J.M., Jeong, J.H., Kim J.M., Joo, K.J. (2001), "A Study on the Reinforcing Efficiency of Short Length H-Shaped Steel Beams with a Rectangular Web Opening", *AIOK.*, **21**(2) 281-284

Acknowledgement

This study was conducted with the support of Personal Basic Research Support Project (NRF-2018R1D 1A1B0704821114) under the sponsorship of National Research Foundation of Korea with funding from the government (Ministry of Education) in 2018. J.M., Joo, K.J. (2001), "A Study on the Reinforcing Efficiency of Short Length H-Shaped Steel Beams with a Rectangular Web Opening", *AIOK.*, **21**(2) 281-284